When **10** is dissolved in acetonitrile-d_3, a superimposed singlet and doublet centered at 0.56 ppm are observed in the ^{31}P NMR spectrum. The $|^1J(PtP)|$ of this resonance indicates that the both phosphines are still coordinated to the platinum in a cis geometry. This suggests that the acetonitrile-d_3 has displaced the water and ether ligands from **10** to form $[cis\text{-}Pt(CD_3CN)_2\{Ph_2P(CH_2CH_2O)_4CH_2CH_2PPh_2\}](BF_4)_2$ (**11**). The exchange of the free and complexed acetonitrile-d_3 would explain the absence of resonances for coordinated acetonitrile-d_3 in the ^{13}C NMR spectrum of **11**.

The exchange of the free and coordinated acetonitrile-d_3 may also explain the fact that all of the phosphorus-coupled resonances in the ^{13}C NMR spectrum of **11** are doublets. Generally, in cis phosphine complexes, these resonances are apparent quintets (A portions of AXX′ spin systems) because of strong phosphorus–phosphorus coupling (large $^2J(XX')$).[34] This is in spite of the fact that the coupling between phosphorus in one ligand and the carbons in the other ligand ($^4J(AX')$) is zero. Exchange of the acetonitriles and the corresponding exchange of the phosphine groups may decouple the two phosphorus nuclei ($J(XX') = 0$). Then, the ^{13}C nuclei in a ligand would be coupled only to the phosphorus nucleus in that ligand, and the ^{13}C resonances would be doublets.

Summary. Ligands of the type $Ph_2P(CH_2CH_2O)_nCH_2CH_2PPh_2$ (n = 3–5) form mononuclear metallacrown ethers with platinum(II). These metallacrown ethers coordinate alkali metal cations in solution, but this is complicated by solubility changes that occur upon complexation and by loss of the chloride ligands. The X-ray crystal structure of $cis\text{-}PtCl_2\{Ph_2P(CH_2CH_2O)_4CH_2CH_2PPh_2\}$ (**5**) suggests that this complex should coordinate most strongly to small cations such as Li^+, while the X-ray crystal structure of $cis\text{-}PtCl_2\{Ph_2P(CH_2CH_2O)_5CH_2CH_2PPh_2\}$ (**6**) suggests that this complex should most strongly coordinate to larger cations such as Na^+. These results are consistent with our earlier studies of $cis\text{-}Mo(CO)_4\{Ph_2P(CH_2CH_2O)_nCH_2CH_2PPh_2\}$ metallacrown ethers.

The most interesting aspect of this work is the observation that the water molecule in the cationic $[Pt\{Ph_2P(CH_2CH_2O)_nCH_2CH_2PPh_2\}(H_2O)](BF_4)_2$ complex (**10**) is both coordinated to the platinum through the oxygen and hydrogen bonded to two of the ether oxygens of the metallacrown ether ring. This suggests that other ligands such as hydroxide, ammonia, and hydroxycarbonyl, which are capable of both coordination and hydrogen bonding, could be incorporated into similar metallacrown ether complexes. Thus, metallacrown ether complexes may be useful as catalysts for the activation of these small molecules.

Acknowledgment. This work was supported by the donors of the Petroleum Research Fund, administered by the American Chemical Society, and by a generous loan of Pt salts by Johnson Mathey. A.V. thanks the graduate school of the University of Alabama at Birmingham for a Graduate Fellowship. We also greatly appreciate the help of Simon Bott (Chemistry Department of the University of North Texas), Kay Fair (Enraf-Nonius), and Fred Fish (Chemistry Department of the University of Alabama at Birmingham) with the solution and refinement of the X-ray crystal structure of **10**.

Supplementary Material Available: Tables of crystallographic data, thermal parameters, calculated hydrogen positions, other bond lengths and angles, and least-squares planes of the phenyl rings in **5**, **6a**, and **10** (14 pages); tables of observed and calculated structure factors for **5**, **6a**, and **10** (100 pages). Ordering information is given on any current masthead page.

(34) Redfield, D. A.; Nelson, J. H.; Cary, L. W. *Inorg. Nucl. Chem. Lett.* **1974**, *10*, 727.
(35) Johnson, C. F. *ORTEP: A Fortran Thermal-Ellipsoid Program for Crystal Structure Illustrations*; Report ORNL-3974, revised; Oak Ridge National Laboratory: Oak Ridge, TN, 1965.

Contribution from the Centre for Magnetic Resonance, The University of Queensland, Queensland 4072, Australia, Department of Chemistry, Section of Inorganic and Analytical Chemistry, University of Ioannina, 45110 Ioannina, Greece, and NRPCS Demokritos, Institute of Material Science, 15310 Aghia Paraskevi Attikis, Greece

Oxovanadium(IV)–Amide Binding. Synthetic, Structural, and Physical Studies of {*N*-[2-(4-Oxopent-2-en-2-ylamino)phenyl]pyridine-2-carboxamido}oxovanadium(IV) and {*N*-[2-(4-Phenyl-4-oxobut-2-en-2-ylamino)phenyl]pyridine-2-carboxamido}oxovanadium(IV)

Graeme R. Hanson,[1a] Themistoklis A. Kabanos,*[1b] Anastasios D. Keramidas,[1b] Dimitris Mentzafos,[1c] and Aris Terzis[1c]

Received October 11, 1991

The complexes [VO(pycac)] and [VO(pycbac)] were prepared by the reaction of bis(pentane-2,4-dionato)oxovanadium(IV) with either *N*-[2-(4-oxopent-2-en-2-ylamino)phenyl]pyridine-2-carboxamide (H_2pycac) or *N*-[2-(4-phenyloxobut-2-en-2-ylamino)-phenyl]pyridine-2-carboxamide (H_2pycbac) in a methanolic solution. Crystals of [VO(pycac)] crystallized from nitromethane were monoclinic, space group $P2_1/n$ with a = 7.5938 (1) Å, b = 30.161 (1) Å, c = 13.6982 (2) Å, β = 86.468 (1)°, Z = 8, and R_w = 5.39%. Crystallization of [VO(pycac)] from chlorobenzene yielded triclinic crystals with a space group $P\bar{1}$ and a = 7.8558 (5) Å, b = 12.934 (1) Å, c = 15.675 (1) Å, α = 78.594 (2)°, β = 89.938 (2)°, γ = 88.097 (2)°, Z = 4, and R_w = 6.45%. [VO(pycbac)] crystals were monoclinic, space group $P2_1/c$ with a = 6.5422 (4) Å, b = 14.4786 (8) Å, c = 19.963 (1) Å, β = 93.461 (2)°, Z = 4, and R_w = 3.80%. The geometry about vanadium in each structure approximates a square pyramid with an average V=O bond length of 1.595 Å with the metal ion 0.669 Å above the basal plane. The average V–N(pyridine), V–N(amine), V–N(amide), and V–O bond lengths are 2.100, 2.045, 1.981, and 1.916 Å, respectively. The V–N(amide) and V–O bond lengths constitute rare examples of such short V–N and V–O distances that have been reported for oxovanadium(IV) complexes to date. In addition to the synthesis and crystallographic studies, we report the optical, infrared, magnetic, electron paramagnetic resonance, and electrochemical properties of these complexes. This study represents the first systematic study of oxovanadium containing a vanadium–amide bond.

Introduction

The discovery of vanadium in biomolecules, such as marine algal bromoperoxidase[2,3] nitrogenase from *Azotobacter vinelandii*,[4,5] marine ascidians,[6] and crude oils[7] has produced considerable interest in its biological function.[8] Vanadium may also prove to be a useful therapeutic agent for the treatment of various

* Author to whom correspondence should be addressed.

(1) (a) Centre for Magnetic Resonance, The University of Queensland. (b) Department of Chemistry, Section of Inorganic and Analytical Chemistry, University of Ioannina. (c) NRPCS Demokritos, Institute of Material Science.

0020-1669/92/1331-2587$03.00/0

diseases, such as diabetes,[9-11] sickle cell anaemia,[12] and cancer.[13] In contrast to iron-, copper-, zinc-, molybdenum-, and nickel-containing metalloproteins, our understanding of the structural, functional, and mechanistic properties of vanadium in metalloproteins is still in its infancy.[8,14] In order to gain an insight into the biological role of vanadium in metalloproteins, it is advantageous to acquire information on its basic coordination chemistry with biologically relevant ligands.

Interactions of oxovanadium(IV) and vanadate with proteins may provide the key to our understanding of the biological role of vanadium in vivo and in vitro. Oxovanadium(IV) has been found to bind specifically (tight binding) and nonspecifically (weak binding) to various proteins including bovine serum albumin, carboxypeptidase, nucleases, and phosphatases,[6,15] while vanadate binds nonspecifically to bovine serum albumin.[16] Oxovanadium(IV) and vanadate can potentially interact with amine, amide, hydroxyl and carboxylic acid functionalities on the protein surface. Although the interactions of vanadium with hydroxylic compounds are becoming better understood, little is known about the coordination of nitrogenous ligands to vanadium, in particular, vanadium–amide binding.[17-20] Herein we report the first syntheses and crystallographic, optical, infrared, magnetic, electron paramagnetic resonance (EPR),[21] and electrochemical properties of such complexes as part of an ongoing program into the study of vanadium complexes with nitrogen-rich ligands. A preliminary report of this research has been communicated previously.[22]

Experimental Section

Materials. Bis(pentane-2,4-dionato)oxovanadium(IV), [VO(acac)$_2$],[23] [bis(salicylaldehyde)ethylenediiminato]oxovanadium(IV), [VO(salen)],[24] [bis(acetylacetone)ethylenediiminato]oxovanadium(IV), [VO(acacen)],[25] and (catecholato)bis(1-phenyl-1,3-butanedionato)vanadium(IV), [V(cat)(bzac)$_2$],[26] were prepared by literature procedures. The purity of the above molecules was confirmed by elemental analyses (C, H, N, and V) and infrared spectroscopy. Reagent grade dichloromethane, acetonitrile, nitromethane, and chlorobenzene were dried and distilled over powdered calcium hydride, while tetrahydrofuran was dried and distilled over sodium wire. Tetraethylammonium perchlorate and tetrabutylammonium perchlorate were prepared by the reaction of perchloric acid with tetraethylammonium bromide and tetrabutylammonium iodide, respectively. Tetraethylammonium perchlorate was recrystallized from water twice. Tetrabutylammonium perchlorate was purified by trituration with water (at room temperature), dissolving the solid in a minimal volume of dichloromethane, and precipitating with slow addition of diethyl ether. Synthesis, distillations, crystallization of the complexes, and spectroscopic characterization were performed under high-purity argon using standard Schlenk techniques.

C, H, and N analyses were performed by the Imperial College, London, Microanalytical Service and vanadium was determined gravimetrically as vanadium pentaoxide.

***N*-(2-Nitrophenyl)pyridine-2-carboxamide (Hpycan).** Pyridine (50 mL) and triphenyl phosphite (186.24 g, 0.60 mol) were added to a mixture of picolinic acid (150.00 g, 1.22 mol) and *o*-nitrophenol (186.24 g, 1.22 mol). The mixture was refluxed for 8 h under vigorous magnetic stirring. The resulting solution was refrigerated overnight at 0 °C yielding a brown-yellow precipitate. The precipitate was filtered off and washed with cold ethanol (4 × 200 mL) and diethyl ether (4 × 200 mL). The product was recrystallized from acetone (twice) to give 85.00 g (28%) of yellow needles which were dried in vacuo over P_4O_{10}. Mp 167 °C. Anal. Calcd for $C_{12}H_9N_3O_3$: C, 59.26; H, 3.73; N, 17.28. Found: C, 59.21; H, 3.70; N, 17.35. ^{1}H NMR ($CDCl_3$, 250 MHz): δ 9.76 (s, 1 H, CONH), 8.88–7.26 (mt, 8 H, aromatic H). ^{13}C NMR ($CDCl_3$, 250 MHz): δ 163.39, 149.64, 148.60, 137.49, 135.43, 134.60, 126.79, 125.78, 123.23, 122.70, 122.20. Mass spectrum (MS): *m/e* 243 [M]. R_f 0.55 (4:1 chloroform/*n*-hexane).

***N*-(2-Aminophenyl)pyridine-2-carboxamide (Hpyca).** To a suspension of Hpycan (60.00 g, 0.25 mol) and 9.00 g of hydrogenation catalyst (10% Pd on activated carbon) in acetone (600 mL), pure hydrogen was admitted for 12 h with vigorous magnetic stirring. The reaction product was separated from the catalyst by filtration and the filtrate was evaporated to dryness to yield a yellow-brown oil. The oil was dissolved in a minimum volume of dichloromethane (100 mL) and *n*-hexane slowly added under vigorous magnetic stirring until a slight precipitate formed. This solution was refrigerated (−20 °C) overnight to yield a yellow precipitate. The precipitate was filtered off, washed with *n*-hexane (2 × 200 mL) and dried in vacuo over P_4O_{10}. A second crop of the product was also obtained by adding to the filtrate *n*-hexane (until a slight precipitate formed) and leaving the solution in the refrigerator (−20 °C) for 2 days. This gave a combined yield of 50.00 g (94%). Mp 94 °C. Anal. Calcd for $C_{12}H_{11}N_3O$: C, 67.59; H, 5.20; N, 15.71. Found: C, 67.62; H, 5.13; N, 15.60. ^{1}H NMR ($CDCl_3$, 250 MHz): δ 9.88 (s, 1 H, CONH), 8.62–6.83 (mt, 8 H, aromatic H), 3.89 (sb, 2 H, NH_2). ^{13}C NMR ($CDCl_3$, 250 MHz): δ 162.31, 149.99, 148.07, 140.25, 137.40, 126.64, 126.22, 124.51, 122.40, 119.47, 117.93. MS: *m/e* 213 [M]. R_f 0.1 (4:1 chloroform/*n*-hexane).

***N*-[2-(4-Oxopent-2-en-2-ylamino)phenyl]pyridine-2-carboxamide (H_2pycac).** A solution of methanol-containing Hpyca (3.50, 16.40 mmol) and pentane-2,4-dione (1.81 g, 18.05 mmol) was refluxed under argon for 3 days. The solution was evaporated to dryness and the residue refluxed with *n*-hexane (200 mL) for 1 h. The hot solution was filtered off and the filtrate refrigerated (−20 °C) overnight. The off-white crystals were filtered off, washed with *n*-hexane (3 × 10 mL) and recrystallized (twice) from *n*-hexane. Yield 3.45 g (71%). Mp 87 °C. Anal. Calcd for $C_{17}H_{17}N_3O_2$: C, 69.14; H, 5.80; N, 14.22. Found: C, 69.25; H, 5.75; N, 14.30. ^{1}H NMR ($CDCl_3$, 250 MHz): δ 12.04 (s, 1 H, NH), 10.38 (s, 1 H, CONH), 8.62–7.10 (mt, 8 H, aromatic H), 5.27 (s, 1 H, COCH), 2.13 (s, 3 H, CH_3CO), 1.76 (s, 3 H, CH_3C=). ^{13}C NMR ($CDCl_3$, 250 MHz): δ 195.94, 161.41, 160.96, 148.91, 147.60, 136.91, 133.91, 128.03, 127.32, 125.90, 123.58, 121.56, 120.29, 97.58, 28.59, 18.70. MS: *m/e* 295 [M]. R_f 0.14 (4:1 chloroform/*n*-hexane).

***N*-[2-(4-Phenyl-4-oxobut-2-en-2-ylamino)phenyl]pyridine-2-carboxamide (H_2pycbac).** A solution of methanol (30 mL) containing Hpyca (3.50 g, 16.41 mmol) and 1-phenylbutane-1,3-dione (2.93 g, 18.05 mmol) was refluxed under argon for 5 days and refrigerated (−20 °C) overnight to produce yellow needles. The crystalline material was filtered off,

(2) Vilter, H. *Phytochemistry* **1984**, *23*, 1387.
(3) De Boer, E.; Van Kooyk, Y.; Tromp, M. G.; Plat, H.; Wever, R. *Biochim. Biophys. Acta* **1986**, *869*, 48.
(4) De Boer, E.; Boon, K.; Wever, R. *Biochemistry* **1988**, *27*, 1629.
(5) Hales, B. J.; Case, E. E.; Morningstar, J. E.; Dzeda, M. F.; Mauterer, L. A. *Biochemistry* **1986**, *25*, 7251.
(6) Chasteen, N. D. *Struct. Bonding (Berlin)* **1983**, *53*, 105.
(7) Reynolds, J. G.; Gallegos, E. T.; Fish, R. M.; Komlenic, J. J. *Energy Fuels* **1987**, *1*, 36.
(8) *Vanadium in Biological Systems: Physiology and Biology*; Chasteen, N. D., Ed.; Kluwer Academic Publishers: Dordrecht, 1990.
(9) Heyliger, C. E.; Tahiliani, A. G.; McNeill, J. H. *Science* **1985**, *227*, 1474.
(10) Meyerovitch, J.; Farfel, Z.; Sack, J.; Schechter, Y. *J. Biol. Chem.* **1987**, *262*, 609.
(11) Tracey, A. S.; Gresser, M. J. *Proc. Natl. Acad. Sci. U.S.A.* **1986**, *83*, 609.
(12) Stankiewicz, P. J.; Gresser, M. J.; Tracey, A. S.; Hass, L. F. *Biochemistry* **1987**, *26*, 1264.
(13) Djordjevic, C.; Wampler, G. L. *J. Inorg. Biochem.* **1985**, *25*, 51.
(14) Bonandies, J. A.; Butler, W. M.; Perocano, V. L.; Carrano, C. J. *Inorg. Chem.* **1987**, *26*, 1218.
(15) Chasteen, N. D. In *Biological Magnetic Resonance*; Berliner, L., Reuben, J., Eds.; Plenum Press: New York, 1981; Vol. 3, p 53.
(16) (a) Arora, J. P. S.; Singh, R. P.; Soam, D.; Kumar, R. *Bioelectrochem. Bioenerg.* **1983**, *10*, 289. (b) Arora, J. P. S.; Singh, R. P.; Soam, D.; Sharma, R. *Bioelectrochem. Bioenerg.* **1983**, *10*, 57.
(17) Rehder, D.; Weideman, C.; Duch, A.; Priebsch, W. *Inorg. Chem.* **1988**, *27*, 584.
(18) Rehder, D. *Inorg. Chem.* **1988**, *27*, 4312.
(19) Crans, D. C.; Bunch, R. L.; Theisen, L. A. *J. Am. Chem. Soc.* **1989**, *111*, 7597.
(20) Redher, D.; Holst, H.; Quaas, R.; Hinrichs, W.; Hahn, U.; Saenger, W. *J. Inorg. Biochem.* **1989**, *37*, 141.
(21) Abbreviations: CV, cyclic voltammetry; EPR, electron paramagnetic resonance; MS, mass spectrum; NMR, nuclear magnetic resonance; acac$^-$, pentane-2,4-dionate; bzac$^-$, 1-phenylbutane-1,3-dionate; acacen^{2-}, bis(acetylacetone)ethylenediiminato; bpy, 2,2′-bipyridine; cat^{2-}, catecholate; edt^{2-}, ethane-1,2-dithiolate; salen^{2-}, bis(salicylaldehyde)-ethylenediiminate; tsalphen^{2-}, *N,N′-o*-phenylenebis(salicylideneiminate); tsaltn^{2-}, *N,N′*-trimethylenebis(thiosalicylideneiminate).
(22) Kabanos, T. A.; Keramidas, A. D.; Mentzafos, D.; Terzis, A. *J. Chem. Soc., Chem. Commun.* **1990**, 1664.
(23) Rowe, R. A.; Jones, M. M. *Inorg. Synth.* **1957**, *5*, 113.
(24) Pasquali, M.; Marcetti, F.; Floriani, C.; Merlino, S. *J. Chem. Soc., Dalton Trans.* **1977**, 139.
(25) Seangprasertkij, R.; Riechel, T. L. *Inorg. Chem.* **1984**, *23*, 991.
(26) Hawkins, C. J.; Kabanos, T. A. *Inorg. Chem.* **1989**, *28*, 1084.

Table I. Crystallographic Data for the Various Oxovanadium(IV) Complexes

compound	[VO(pycac)][a]	[VO(pycac)][b]	[VO(pycbac)]
formula	$C_{17}H_{15}N_3O_3V$	$C_{17}H_{15}N_3O_3V$	$C_{22}H_{17}N_3O_3V$
fw	360.27	360.27	422.34
cryst solvent	nitromethane	chlorobenzene	nitromethane
space group	$P2_1/n$	$P\bar{1}$	$P2_1/c$
cryst dimens, mm	0.23 × 0.6 × 0.12	0.22 × 0.18 × 0.3	0.08 × 0.18 × 0.39
a, Å	7.5938 (1)	7.8558 (5)	6.5422 (4)
b, Å	30.161 (1)	12.934 (1)	14.4786 (8)
c, Å	13.6982 (2)	15.675 (1)	19.963 (1)
α, deg		78.594 (2)	
β, deg	86.468 (1)	89.938 (2)	93.461 (2)
γ, deg		88.097 (2)	
V, Å^3	3131.5 (1)	1560.4 (1)	1887.5 (1)
Z	8	4	4
d_{calc}, g cm^{-3}	1.528	1.533	1.486
d_{obs}, g cm^{-3}	1.52	1.52	1.47
cryst color	red-brown	red-brown	red-brown
μ, cm^{-1}	63.50	63.37	53.55
max abs cor factor	1.17	1.06	1.22
2θ range, deg	130	130	122
no. of data collcd/unique	5861/5298	5555/5298	3325/2892
no. of data used	4400	4738	2496
with $F_o \geq$	$4.0\sigma(F_o)$	$6.0\sigma(F_o)$	$4.0\sigma(F_o)$
range of h,k,l	±8, 35, 16	±9, ±15, 18	±7, 16, 22
R_{int}	0.0253	0.0245	0.024
weighting scheme	$1/w = \sigma^2(F_o) + gF^2_o$		
	$g = 0.00013$	$g = 0.00018$	unit weights
no. of parameters	521	537	273
$\lvert\Delta/\sigma\rvert_{max}$	0.389	0.345	0.107
residual extreme in final diff map, Å^{-3}	0.350, −0.297	0.431, −0.352	0.300, −0.222
quality of fit indicator[c]	2.09	4.37	1.02
R,[d] obsd	0.0378	0.0407	0.0366
R_w,[e] obsd	0.0539	0.0645	0.0380

[a] a-form. [b] b-form. [c] Quality of fit indicator = $[\sum w(\lvert F_o\rvert - \lvert F_c\rvert)^2/(N_{observ} - N_{params})]^{1/2}$. [d] $R = \sum\lvert\Delta F\rvert/\sum\lvert F_o\rvert$. [e] $R_w = [\sum w(\Delta F)^2/\sum w\lvert F_o\rvert^2]^{1/2}$.

washed with diethyl ether, and recrystallized (twice) from methanol. Yield 5.50 g (94%) of yellow crystals. Mp 127.5 °C. Anal. Calcd for $C_{22}H_{19}N_3O_2$: C, 73.93; H, 5.36; N, 11.76. Found: C, 73.85; H, 5.30; N, 11.85. ^{1}H NMR ($CDCl_3$, 250 MHz): δ 12.70 (s, 1 H, NH), 10.51 (s, 1 H, CONH), 8.68–7.10 (m, 13 H, aromatic H), 6.05 (s, 1 H, COCH), 1.96 (s, 3 H, CH_3). ^{13}C NMR ($CDCl_3$, 250 MHz): δ 188.90, 163.65, 161.87, 149.19, 147.92, 139.47, 137.21, 134.19, 130.83, 128.22, 128.05, 127.93, 127.63, 126.88, 126.18, 123.97, 121.87, 120.60, 94.31, 19.68. MS: m/e 355 [M]. R_f 0.24 (4:1 chloroform/n-hexane).

{*N*-[2-(4-Oxopent-2-en-2-ylamino)phenyl]pyridine-2-carboxamido}-oxovanadium(IV), [VO(pycac)]. H_2pycac (1.20 g, 4.06 mmol) was added slowly to a stirred solution of bis(pentane-2,4-dionato)oxovanadium(IV) (1.00 g, 3.77 mmol) in methanol (35 mL). This produced a color change from blue-green to green. The solution was refluxed under argon for 3 days after which the color of the solution changed to brown and a brown precipitate formed. The hot solution was cooled to room temperature and filtered, and the precipitate was washed with methanol (3 × 20 mL) and diethyl ether (2 × 30 mL) and dried in vacuo over P_4O_{10}: yield, 0.60 g (45%); mp 240 °C (dec). Crystals of [VO(pycac)] (a- and b-forms) were obtained by slow cooling of a hot concentrated solution of the complex in either chlorobenzene or nitromethane. Anal. Calcd for $C_{17}H_{15}N_3O_3V$: C, 56.67; H, 4.20; N, 11.66; V, 14.14. Found: C, 56.50; H, 4.15; N, 11.70; V, 14.25. MS: m/e 362 [M + 2], 361 [M + 1], 360 [M]. R_f 0.07 (4:1 chloroform/n-hexane). Electronic spectra (λ, nm; ϵ, M^{-1} cm^{-1}, dichloromethane): 660 sh, 30; 345, 11 230; 284 sh, 9100; 261, 20 250; 221, 20 470.

{*N*-[2-(4-Phenyl-4-oxobut-2-en-2-ylamino)phenyl]pyridine-2-carboxamido}oxovanadium(IV), [VO(pycbac)]. The complex was prepared as described above except the solution was refluxed for 1 day: yield, 94%; mp 290 °C (dec). Crystals of [VO(pycbac)] were obtained by slow cooling of a hot concentrated solution of the complex in nitromethane. Anal. Calcd for $C_{22}H_{17}O_3N_3V$: C, 62.57; H, 4.06; N, 9.95; V, 12.06. Found: C, 62.47; H, 3.98; N, 10.01; V, 12.00. MS: m/e 424 [M], 423 [M − 1], 422 [M − 2]. R_f 0.07 (4:1 chloroform/n-hexane). Electronic spectra (λ, nm; ϵ, M^{-1} cm^{-1}, dichloromethane): 685 sh, 43; 395, 14 140; 364, 14 320; 288 sh, 10 560; 260, 26 350; 220, 23 800.

These oxovanadium(IV) complexes are stable toward aerial oxidation in the solid state but decompose slowly in solution.

Spectroscopic Techniques. Infrared spectra of the various compounds dispersed in KBr pellets were recorded on a Perkin-Elmer 577 spectrometer. A polystyrene film was used to calibrate the frequency. Electronic absorption spectra were measured as solutions in septum-sealed quartz cuvettes on a Phillips PU8740 spectrophotometer. ^{1}H and ^{13}C NMR were measured on a Bruker WM250 spectrometer. Electron impact and fast atom bombardment (FAB) mass spectra were measured on a VG 2020 instrument. A thiodiethanol matrix was employed for the FAB measurements.

X-ray Diffraction Data Collection, Structure Solution, and Refinement. A summaries of crystal and intensity collection data are given in Table I. The crystal systems and the space groups were revealed by preliminary oscillation and Weissenberg photographs. Diffraction measurements were made on a Syntex $P2_1$ diffractometer upgrated by Crystal Logic, with Ni-filtered Cu Kα radiation, λ = 1.5418 Å. The cell constants were determined and refined by using the angular settings of 40 automatically centered reflections in the range $23° < 2\theta < 53°$. Intensity data were recorded using θ–2θ scan, at 298 K. Three reflections monitored periodically every 97 reflections showed <3.0% intensity fluctuation. Lorenz, polarization and Ψ-scan absorption corrections were applied using Crystal Logic (UCLA package) software. The structures were solved by direct methods and the refinement, based on F, proceeded with SHELX76[27] by minimizing $\sum w\Delta^2$. All hydrogen atoms were located from difference Fourier maps, but because of an insufficient number of reflections, the positions of the methyl hydrogen atoms were not refined in [VO(pycac)] (a- and b-forms) and only H(14) was refined in [VO(pycbac)]. The hydrogens that were nonrefined were placed at calculated positions as riding on carbon atoms at a 1.08 Å distance. The non-H atoms were refined anisotropically and the H-atoms isotropically. Unit weights were used in [VO(pycbac)] since they gave a satisfactory analysis of variance. Atomic scattering factors were from ref 28.

Electrochemistry. Electrochemical experiments were performed with a Metrohm E614 Polarecord-VA-Scanner E612 apparatus connected to a Houston 2000 XY recorder. Glassy carbon disk and dropping mercury electrodes (DME) were employed as working electrodes for the cyclic voltammetric and polarographic studies, respectively. A platinum wire was used as an auxiliary electrode, while a calomel electrode in dichloromethane (saturated with tetrabutylammonium perchlorate) or acetonitrile (saturated with tetraethylammonium perchlorate) was used as a reference electrode. The supporting electrolyte in dichloromethane

(27) Shelrick, G. H. SHELX76. A program for Crystal Structure Determination. University of Cambridge, U.K., 1976.
(28) *International Tables For X-ray Crystallography*; Kynoch Press: Birmingham, 1974; Vol. IV.

Table II. Interatomic Distances (Å) and Angles (deg) Relevant to the Vanadium Coordination Sphere

	[VO(pycac)][a]		[VO(pycac)][b]		
parameter	molecule 1	molecule 2	molecule 1	molecule 2	[VO(pycbac)]
V–O(1)	1.599 (2)	1.590 (2)	1.592 (2)	1.598 (2)	1.596 (2)
V–O(3)	1.916 (2)	1.912 (2)	1.936 (2)	1.904 (2)	1.913 (2)
V–N(1)	2.097 (2)	2.109 (2)	2.091 (2)	2.110 (2)	2.095 (2)
V–N(2)	1.984 (2)	1.983 (2)	1.970 (2)	1.978 (2)	1.989 (2)
V–N(3)	2.052 (2)	2.048 (2)	2.042 (2)	2.045 (2)	2.037 (2)
N(1)–V–O(1)	107.1 (1)	107.5 (1)	106.3 (1)	107.2 (1)	106.2 (1)
N(2)–V–O(1)	111.6 (1)	110.7 (1)	111.4 (1)	110.8 (1)	108.9 (1)
N(2)–V–N(1)	77.6 (1)	77.3 (1)	78.1 (1)	77.4 (1)	77.8 (1)
N(3)–V–O(1)	106.9 (1)	108.4 (1)	106.9 (1)	107.0 (1)	108.6 (1)
N(3)–V–N(1)	143.8 (1)	142.0 (1)	144.7 (1)	143.5 (1)	142.9 (1)
N(3)–V–N(2)	78.6 (1)	78.8 (1)	79.1 (1)	79.0 (1)	79.1 (1)
O(3)–V–O(1)	112.3 (1)	111.3 (1)	111.4 (1)	112.3 (1)	110.6 (1)
O(3)–V–N(1)	88.4 (1)	88.1 (1)	89.0 (1)	88.5 (1)	89.0 (1)
O(3)–V–N(2)	136.1 (1)	137.9 (1)	137.2 (1)	136.9 (1)	140.5 (1)
O(3)–V–N(3)	90.1 (1)	90.2 (1)	89.7 (1)	90.1 (1)	90.6 (1)

[a] a-form. [b] b-form.

and acetonitrile was tetrabutylammonium perchlorate and tetraethylammonium perchlorate (0.1 M), respectively, and all solutions were 10^{-3}–10^{-4} M in complex. Values for the reduction potential ($E_{1/2}$) and the number of electrons involved in the reversible process were obtained from the intercept and the slope of the plot of ln $[(i_d - i)/i]$ versus potential (E) according to the Heyrovsky–Ilkovic equation[29]

$$E = E_{1/2} + (RT/nF) \ln [(i_d - i)/i] \quad (1)$$

All potentials throughout this paper are relative to the normal hydrogen electrode (NHE)[30] using ferrocene (+0.400 V vs NHE)[31] as a standard.

Magnetism and EPR Spectroscopy. Magnetic moments were measured at room temperature by the Faraday method, with mercuric tetrathiocyanatocobaltate(II) as the susceptibility standard on a Cahn-Ventron RM-2 balance.

X-Band (ca. 9.12 GHz) EPR spectra, recorded as the first derivative of absorption, were obtained by using a Bruker ER-200D EPR spectrometer.[32] A Bruker (VT-100) flowthrough variable temperature controller provided temperatures of 120–140 K at the sample position in the cavity. Calibration of the microwave frequency and the magnetic field were performed with an EIP 845A microwave frequency counter and a Bruker 035M gaussmeter, respectively. Simulation of the monomeric oxovanadium(IV) EPR signal (S), measured as a function of magnetic field (B) and at a constant frequency (ν_c), was performed using eq 2,[33] where the constant, C, involves experimental parameters, $\bar{g}_1^2$ is

$$S(\nu_c,B) = C \sum_{\varphi=0}^{\pi/2} \sum_{\phi=0}^{\pi/2} \sum_{M_I=-7/2}^{7/2} \bar{g}_1^2 f(\nu_c - \nu_o(B),\sigma_\nu)\Delta \cos\theta \Delta\phi \quad (2)$$

the powder averaged expression for the transition probability,[34] and f is the Gaussian lineshape function. In f, $\nu_o(B)$ is the actual energy difference between the energy levels and is evaluated with second-order perturbation theory.[35,36] The fundamental reason for using eq 2 is given elsewhere.[37]

The actual line width in frequency units is

$$\sigma_i^2 = \sigma_{R_i}^2 + [C_1\nu_o(B) - C_2M_1]^2 \quad (3)$$

where i corresponds to the principal directions ($i = x, y, z$) in the molecule. The σ_R's are residual line widths, due to dipolar broadening and/or unresolved metal and ligand hyperfine interactions while the C_1 and C_2's represent strain-induced distributions of the g- and A-values. The angular variation, for purposes of frozen solution spectral simulations, is assumed to behave in an analogous manner to hyperfine structure, viz.

$$\sigma_\nu^2 = \sum_{i=x,y,z} g_i^2 l_i^2 \sigma_i^2 \quad (4)$$

where l_i is the direction cosine relating the applied magnetic field to the principal axes.

In all cases spectral fits were refined using an automatic least-squares fitting program EPR50FIT on the University of Queensland's Prentice Computer Centre's (PCC's) IBM 3081 computer. The quality of the final simulated spectrum can be estimated from the least-squares error parameter (LSE).[38] Spectral subtractions, comparisons, and the determination of LSE were carried out with the EPR software package EPR_PLOT running on the PCC's VAX 8550 computer

$$\mathrm{LSE} = \sum_{i=1}^{N_{pts}} (E_i/I_E - S_i/I_S)^2/N_{pts} \quad (5)$$

where I_E and I_S are the normalization factors (doubly integrated intensities) and N_{pts} is the number of points in both the simulated (S) and the experimental (E) spectra.

Results and Discussion

Syntheses. *N*-(2-Nitrophenyl)pyridine-2-carboxamide (Hpycan) was prepared by a highly efficient and more convenient method[39] than that described by Kabanos et al.[40] *N*-(2-Aminophenyl)pyridine-2-carboxamide (Hpyca) was prepared by a modification of the method used by Kabanos et al.[40] The ligands H_2pycac and H_2pycbac were prepared by condensing Hpyca with either pentane-2,4-dione or 1-phenylbutane-1,3-dione. The synthesis of the organic molecules Hpycan and Hpyca and the ligands H_2pycac and H_2pycbac used in the synthesis of the oxovanadium(IV) complexes is depicted in Scheme I. The method of ligand substitution was employed for the preparation of the oxovanadium(IV) complexes

$$[VO(acac)_2] + H_2pycac \rightarrow [VO(pycac)] + 2Hacac \quad (6)$$

All of the reactions were followed by thin-layer chromatography. The peaks in the infrared spectra of H_2pycac, H_2pycbac, and their corresponding oxovanadium(IV) complexes are fully listed in Table S7, supplementary material. The spectrum of H_2pycac exhibits the ν(NH), amide I [+ν(C=O) ketone], ν(C=C), amide II, and amide III modes at 3322, 1677, 1580, 1520, and 1223 cm^{-1} respectively. The corresponding bands for H_2pycbac occur at 3321, 1673, 1572, 1515, and 1225 cm^{-1}. Differences between the spectra of the ligands and oxovanadium(IV) complexes are readily observable. Importantly, the ν(NH) bands are absent in the spectra of [VO(pycac)] and [VO(pycbac)], as expected from the stoichiometry. In addition the amide II and III peaks were replaced by a very strong band at 1370 cm^{-1}, which is characteristic for deprotonated secondary amide complexes.[41] This replacement is to be expected, as the removal of an amide proton produces a

(29) Heyrovsky, J.; Ilkovic, D. *Collect. Czech. Chem. Commun.* **1935**, *7*, 198.
(30) Gagne, R. R.; Koval, C. A.; Lisensky, G. C. *Inorg. Chem.* **1980**, *19*, 2854.
(31) Koepp, H. M.; Wendt, H.; Strehlow, H. *Z. Electrochem.* **1960**, *64*, 483.
(32) Acceptable signal to noise ratios were obtained by signal averaging the spectra on a Cleveland personal computer, using the computer program SIMOPR written by R. W. Garret.
(33) Dougherty, G.; Pilbrow, J. R.; Skorobogarty, A.; Smith, D. *J. Chem. Soc., Faraday Trans. 2* **1985**, *81*, 1739.
(34) Pilbrow, J. R. *Mol. Phys.* **1969**, *16*, 307.
(35) Freeman, T. E. Ph.D. Thesis, Monash University, Australia, 1973.
(36) Lin, W. C. *Mol. Phys.* **1973**, *25*, 247.
(37) Pilbrow, J. R. *J. Magn. Reson.* **1984**, *58*, 186.
(38) Martinelli, R. A.; Hanson, G. R.; Thompson, J. S.; Holmquist, B.; Pilbrow, J. R.; Vallee, B. L. *Biochemistry* **1988**, *28*, 2251.
(39) (a) Mitin, Y. V.; Glinskaya, J. V. *Tetrahedron Lett.* **1969**, 5267. (b) Yamazaki, N.; Higashi, F. *Tetrahedron Lett.* **1972**, 5047.
(40) Kabanos, T. A.; Tsangaris, J. M. *J. Coord. Chem.* **1984**, *13*, 89.
(41) Barnes, D. J.; Chapman, R. L.; Stephens, F. S.; Vagg, R. S. *Inorg. Chim. Acta* **1981**, *51*, 155.

Table III. Electrochemical Data: Cyclic Voltammetric and dc Polarographic Studies of Oxovanadium(IV) Complexes[a]

complex	solvent	E_{pc}, V	E_{pa}, V	i_{pc}/i_{pa}	ΔE_p,[b] mV	$E_{1/2}$,[c] V	donor set
[VO(pycac)]	CH_3CN	−1.58	−1.51	1.1	70	−1.54	N_3O
						(−1.50)	
		+0.78	+0.86	1.0	80	+0.82	
	CH_2Cl_2	−1.71	−1.59	1.1	125	−1.65	
						(−1.68)	
		+0.81	+0.94	1.0	120	+0.88	
	THF	−1.85	−1.53	1.1	325	−1.69	
						(−1.72)	
		+0.66	+0.98	0.9	325	+0.82	
[VO(pycbac)]	CH_3CN	−1.86	−1.79	1.0	75	−1.83	N_3O
						(−1.82)	
		−1.46	−1.39	1.0	65	−1.43	
						(−1.45)	
		+0.82	+0.90	0.9	75	+0.86	
	CH_2Cl_2	−1.63	−1.51	1.1	120	−1.57	
						(−1.59)	
		+0.82	+0.94	0.9	120	+0.88	
	THF	−2.14	−1.82	1.1	325	−1.98	
						(−2.09)	
		−1.75	−1.43	1.0	325	−1.59	
						(−1.65)	
		+0.64	+0.96	0.9	325	+0.8	
[VO(salen)][d]	CH_3CN		−1.66				N_2O_2
		+0.43	+0.50	1.0	70	+0.47	
[VO(acacen)][d]	CH_3CN		−1.83				N_2O_2
		+0.51	+0.58	1.0	70	+0.54	

[a] All potentials are relative to NHE. [b] $\Delta E_p = E_{pc} - E_{pa}$ at a scan rate of 100 mV s^{-1}. [c] Values of the redox potentials ($E_{1/2}$) were calculated from the formula $E_{1/2} = 0.5(E_{pc} + E_{pa})$ from cyclic voltammetric measurements, while values in parentheses of the reduction potentials ($E_{1/2}$) were obtained from the intercepts of plots of log $[(i_d - i)/i]$ vs potential (E). [d] Measurements have been repeated here with ferrocene (0.400 V) as reference to give potentials relative to NHE.

Scheme I

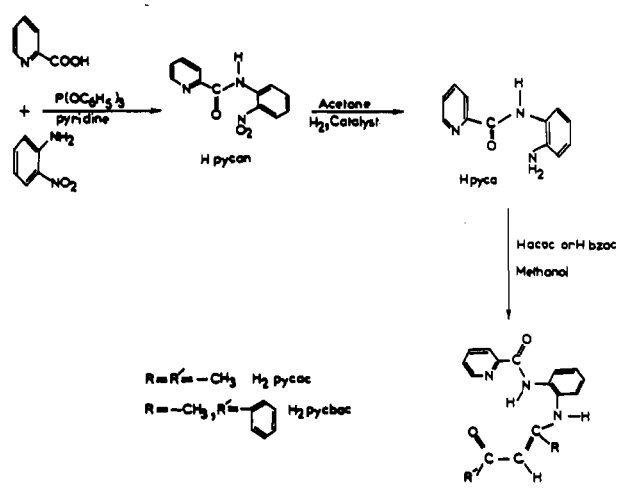

pure C—N vibrational stretching mode. The very strong ν(V=O) band occurs at 984 and 980 cm^{-1} in [VO(pycac)] and [VO(pycbac)], respectively.

Crystallography. A selection of interatomic distances and bond angles relevant to the vanadium coordination sphere in [VO(pycac)] crystallized from either nitromethane (a-form) or chlorobenzene (b-form) and [VO(pycbac)] complexes are listed in Table II. Structures of the two oxovanadium(IV) complexes are shown in Figure 1. Since the bond lengths and angles for the three structures (Table III) are almost identical, it was decided to only describe the structure of [VO(pycbac)]. The coordination environment of the vanadium atom approximates a square pyramid with the oxo ligand in the apical position and the donor atoms of the tetradentate ligand in the basal plane. The four basal atoms are within 0.02 Å of the mean plane with the vanadium atom 0.667 Å above this plane. The V=O bond length (1.596 (2) Å) is in the range 1.56–1.63 Å reported for other square pyramidal oxovanadium(IV) complexes.[42]

The V–O bond length (1.913 (2) Å) constitutes one of the shortest V–O bond distances so far reported for oxovanadium(IV) complexes. Actually, to our knowledge there are only two more examples with slightly shorter V–O bond distances, bis[*N*-(hydroxyethylene)salicylideneaminato]oxovanadium(IV)[43] and bis[*N*-(4-chlorophenyl)salicylideneaminato]oxovanadium(IV)[44] with V–O distances of 1.892 and 1.900 Å, respectively. Previous studies[45,46] have shown that when a phenyl group is adjacent to a ketone-oxygen ligating atom, the corresponding V–O bond length is reduced. This is presumably a consequence of the delocalization of electron density from the chelate ring to the phenyl group.[45] A comparison of the V–O bond lengths (1.914 Å) for [VO(pycac)] and [VO(pycbac)] (1.913 Å) which have methyl and phenyl groups adjacent to the ketone-oxygen, respectively, reveals an insignificant reduction in the V–O bond length. This is despite the fact that the phenyl ring is almost coplanar with the rest of the organic ligand.

Of the three V–N bonds, the bond to N(2) (1.989 (2) Å), the amide nitrogen, is almost identical with the shortest V–N distance (1.97 (1) Å) reported for the oxovanadium(IV) complex {17,18,19,20-tetrahydrotribezo[*e,i,m*][1,4,8,11]tetraazacyclotetradecinato(2−)}oxovanadium(IV).[47] This is in agreement with the fact that the deprotonated amide nitrogen is a very strong σ-donor. According to Bernhardt et al.[48] this may reflect some V=N character due to donation of electron density from the deprotonated amide nitrogen into metal d-orbitals. It is interesting to note that the largest deviation from the best V(1)–N(2)–C(6)–C(7)–O(2) plane is 0.04 Å, which contrasts with other highly oxidized metal ion complexes in which the amide function may be nonplanar.[49] The longer V–N bond lengths to N(1) (2.095

(42) Nugent, W. A.; Mayer, J. M. *Metal-Ligand Multiple Bonds*; John Wiley and Sons: New York, 1988; pp 160–161.
(43) Carrano, C. J.; Nunn, C. N.; Quan, R.; Bonadies, J. A.; Pecorano, V. L. *Inorg. Chem.* **1990**, *29*, 944.
(44) Pasquali, M.; Marchetti, F.; Floriani, C. *J. Chem. Soc., Dalton Trans.* **1977**, 139.
(45) Hon, P. K.; Belford, R. L.; Peluger, C. E. *J. Chem. Phys.* **1965**, *43*, 1323.
(46) Hambley, T.; Hawkins, C. J.; Kabanos, T. A. *Inorg. Chem.* **1987**, *26*, 3740.
(47) Greenwood, A. J.; Henrick, K.; Owston, P. G.; Tasker, P. A. *J. Chem. Soc., Chem. Commun.* **1980**, 88.
(48) Bernhardt, P. V.; Lawrence, G. A.; Comba, B.; Martin, L. L.; Hambley, T. W. *J. Chem. Soc., Dalton Trans.* **1990**, 2859.

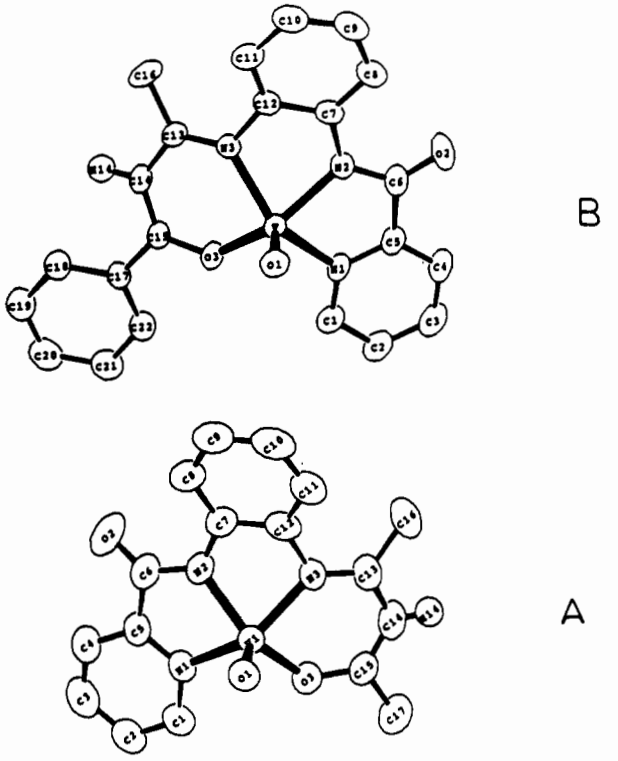

Figure 1. ORTEP drawings of (A) [VO(pycac)] and (B) [VO(pycbac)] at 50% probability ellipsoids giving atomic numbering.

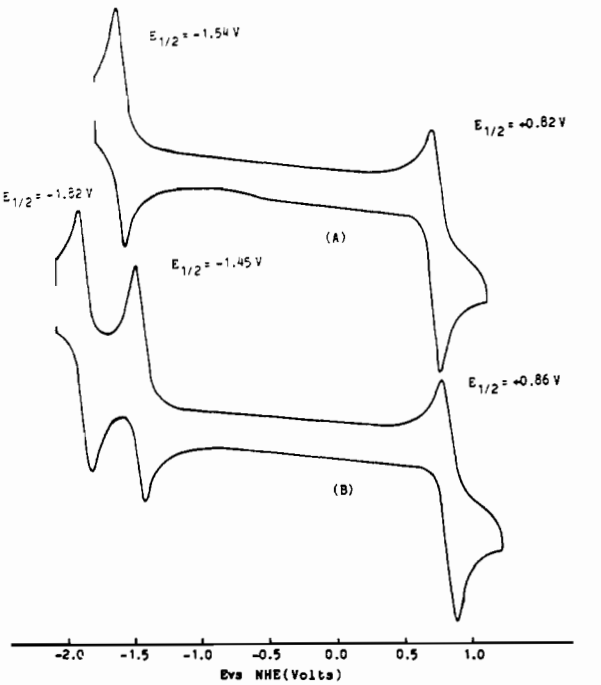

Figure 2. (A) dc cyclic voltammogram for the oxidation and reduction of [VO(pycac)] in MeCN with tetraethylammonium perchlorate (0.1 M) at a glassy carbon electrode and a scan rate of 100 mV s^{-1}. (B) A dc cyclic voltammogram for the oxidation and reductions of [VO(pycbac)] with the same conditions as in voltammogram A.

(2) Å), the pyridine nitrogen, and N(3) (2.037 (2) Å) reflect the changes in donor strengths of the respective nitrogen atoms and are in the range expected for V–N oxovanadium(IV) complexes.

Electrochemistry. The results of the cyclic voltammetric (CV) and dc polarographic studies for the above oxovanadium(IV) complexes in acetonitrile, dichloromethane, and tetrahydrofuran are given in Table III. The dc polarographic investigations in acetonitrile reveal a one-electron reversible redox process at −1.50 V for [VO(pycac)] and two one-electron reversible redox processes at −1.45 and −1.82 V for [VO(pycbac)]. The dc polarographic studies in dichloromethane show one-electron reversible redox processes at −1.68 and −1.59 V for [VO(pycac)] and [VO(pycbac)], respectively, while in tetrahydrofuran a one-electron reversible process occurs at −1.72 V for [VO(pycac)] and two one-electron reversible redox processes occur at −1.65 and 2.09 V for [VO(pycbac)].

The CV examination of the two complexes in acetonitrile reveals the presence of two redox couples for [VO(pycac)] (Figure 2A) and three redox couples for [VO(pycbac)] (Figure 2B). The peak separation (ΔE_p) for each complex is close to that anticipated for a Nernstian one-electron process (59 mV);[50] plots of C_p (peak current) versus $SR^{1/2}$ (SR = scan rate) are linear, and the ratio of the cathodic to anodic peak currents is 1, indicating that electron transfer is reversible and that mass transfer is limited. In tetrahydrofuran two sets of peaks for [VO(pycac)] and three for [VO(pycbac)] are also obtained but the peak separations for all redox couples are 325 mV, indicating irreversible behavior in this solvent. In dichloromethane two sets of peaks are obtained for both complexes with peak-current ratios being unity and the ΔE_p values being 120 mV (ΔE_p for ferrocene under these conditions is 120 mV) and almost independent of scan rate below 500 mV s^{-1}, indicating that both redox processes are reversible. All the redox couples in the three solvents have the same anodic and cathodic peak currents indicating that all electrochemical processes have the same number of electrons, and since the redox couples at negative potentials are one-electron processes (polarography), the redox couples at the positive potentials must also be one-electron processes.

A CV study of the ligands in the potential range −1.90 to +1.60 V in CH_2Cl_2, −2.10 to +1.60 V in CH_3CN and −2.50 to +1.60 V in tetrahydrofuran yields only one peak at ca. +1.4 V due to ligand oxidation. It is interesting to note that while the cyclic voltammogram of [VO(pycbac)] yields three couples of peaks in acetonitrile and two couples in dichloromethane, the cyclic voltammogram of [VO(pycac)] yields two couples of peaks in both solvents. In an effort to clarify the situation, tetrahydrofuran was employed as a solvent; however, results identical to those found in acetonitrile were observed. The suggested electrode reactions are

$$[V^{V}O(pycac)]^{+} + e^{-} \rightleftarrows [V^{IV}O(pycac)] \quad (7)$$

$$E_{1/2,CH_3CN} = +0.78 \text{ V}$$

$$[V^{IV}O(pycac)] + e^{-} \rightleftarrows [V^{III}O(pycac)]^{-} \quad (8)$$

$$E_{1/2,CH_3CN} = -1.50 \text{ V}$$

It is worth noting that to our knowledge [VO(pycac)] and [VO(pycbac)] are the first examples of oxovanadium(IV) exhibiting in organic solvents[48,51] a reversible (in both polarography and CV) one-electron reduction centered on vanadium, and the most striking feature of the CV of [VO(pycbac)] is a further one-electron reversible reduction of [VO(pycbac)]; we are unable to unequivocally assign this process to a V(III) → V(II) reduction, which would be unprecedented, as there is potential for reversible reduction of the ligand. It is obvious that this requires further investigation, and efforts to isolate and characterize the corresponding V(III) and V(II) species are underway.

One of the aims of this study was to see how the redox properties of oxovanadium(IV) complexes were affected by changing the

(49) (a) Collins, T. J.; Coots, R. J.; Fututani, Keech, J. T.; Peake, G. T.; Santrarsiero, B. D. *J. Am. Chem. Soc.* **1986**, *108*, 5333. (b) Collins, T. J.; Gorolon-Wylie, S. W. *J. Am. Chem. Soc.* **1989**, *111*, 4511.

(50) Nicholson, R. S.; Shain, I. *Anal. Chem.* **1964**, *36*, 706.

(51) dc polarography of [6,13-dimethyl-1,4,8,11-tetraazacyclotetradecane-6,13-diamineoxovanadium(IV) perchlorate][57] in aqueous solution reveals one electron reversible behaviour at −0.87 V versus Ag–AgCl. dc cyclic voltammetry revealed a redox couple of waves at −0.89 and −0.66 V versus Ag–AgCl. The large separation of the cathodic and anodic peak potentials (230 mV) was attributed to the protonation of the oxo ligand after reduction of the oxovanadium(IV) complex.

Table IV. Spin Hamiltonian Parameters for Oxovanadium(IV) Complexes with Various Coordination Spheres

compound	donor set	g_z	g_x	g_y	$-A_z$[a]	$-A_x$	$-A_y$	g_{iso}	$-A_{iso}$
$[VO(acac)_2]$[b]	O_4	1.944	1.983	1.987	174	62	60	1.970	99
$[VO(tfacac)_2]$[b]	O_4	1.944	1.982	1.987	174	64	61	1.970	100
[VO(salen)][c]	N_2O_2	1.955	1.986	1.989	166.00	56.00	55.00	1.978	92.33
$[VO(acacen)_2]$[c]	N_2O_2	1.956	1.987	1.987	164	55	55	1.977	92
[VO(pycac)][d,e]	N_3O	1.9558	1.9777	1.9811	151.43	53.29	42.46	1.9772	88.89
[VO(pycbac)][d,f]	N_3O	1.9573	1.9764	1.9812	152.42	53.59	38.26	1.9773	88.56
$[VO(bpy)_2]^{2+}$[g]	N_4	1.948	1.981	1.981	161.19	56.42	56.42	1.970	91.34
[VO(tsaltn)][h]	N_2S_2	1.966	1.975	1.975	140	37	37	1.972	71.33
[VO(tsalphen)][h]	N_2S_2	1.967	1.987	1.987	145	51	51	1.9803	82.33
$[VO(edt)_2]^{2-}$[i]	S_4	1.976	1.978	1.977	133.8	39.7	39.7	1.977	71.1

[a] Units of hyperfine coupling constants, $\times 10^{-4}$ cm^{-1}. [b] References 53 and 55. [c] Reference 55. [d] Measured in chloroform at 120 K. [e] LSE values for the isotropic and anisotropic computer simulations are 9.719×10^{-3} and 1.669×10^{-3}, respectively. [f] LSE values for the isotropic and anisotropic computer simulations are 9.262×10^{-3} and 9.303×10^{-4}, respectively. [g] Reference 56. [h] Reference 57. [i] Reference 52.

Table V. Line Width Parameters for [VO(pycac)] and [VO(pycbac)]

compound	σ_{R_z}[a]	σ_{R_x}	σ_{R_y}	C_{1z}	C_{1x}	C_{1y}	C_{2z}[a]	C_{2x}	C_{2y}
[VO(pycac)]	18.027	7.898	9.655	0.0011	0.0000	0.0000	17.041	2.826	1.670
[VO(pycbac)]	20.604	8.942	10.769	0.0053	−0.0016	0.0003	17.568	2.863	1.668

[a] Units for σ_R and C_2 are MHz.

in-plane donor atoms from N_2O_2 to N_3O. The potential data (Table III) for [VO(salen)], [VO(acacen)], [VO(pycac)], and [VO(pycbac)] reveal that the oxidation of complexes with a N_2O_2 donor set is easier than for complexes with N_3O donor set. This is probably a consequence of the presence of a larger number of ligating nitrogen atoms which do not exhibit a strong preference for coordination[14] to VO^{3+} relative to VO^{2+}. Conversely it is thermodynamically easier to reduce [VO(pycac)] and [VO(pycbac)] to the V(III) state.

Magnetism and Electron Paramagnetic Spectra. The magnetic moments of [VO(pycac)] and [VO(pycbac)] are 1.72 and 1.76 μ_B, respectively, at 298 K in accord with the spin-only value expected for d^1, $S = {}^1/_2$ systems.

The isotropic (liquid solution) EPR spectra of these oxovanadium(IV) complexes reveal eight resonances attributable to a single $S = {}^1/_2$ species in which the unpaired electron in a d_{xy} orbital is coupled to the nuclear spin of the vanadium nucleus (^{51}V, 99.76 atom %, $I = {}^7/_2$, $\mu = 5.149\ \beta_N$). These results are consistent with the magnetic moments and show that ligand dissociation has not occurred during the preparation of the EPR samples.

The anisotropic EPR spectra of the distorted square pyramidal d^1 anions [VO(pycac)] (Figure 3A) and [VO(pycbac)] can be described by an orthorhombic spin Hamiltonian

$$\mathcal{H} = \beta \sum_{i=x,y,z} g_i B_i S_i + S_i A_i I_i \qquad (9)$$

where the parameters have their usual definitions. The spin Hamiltonian and line width parameters (σ_{R_i}, C_{1_i}, and C_{2_i}; Tables IV and V) for the two oxovanadium(IV) complexes prepared in this study were determined by computer simulation of the experimental EPR spectrum (eq 2, Figure 3B). A comparison of the g- and A-matrices for [VO(pycac)] and [VO(pycbac)] with those from oxovanadium(IV) complexes with different equatorial ligand field strengths: $VO(O_4)$, $VO(N_2O_2)$, $VO(N_4)$, $VO(N_2S_2)$, and $VO(S_4)$ (Table IV) reveals several interesting features. Firstly, the magnitudes of A_x and A_y are significantly smaller than the values for other oxygen and nitrogen donor complexes. In fact their magnitude is comparable to complexes with either sulfur or nitrogen/sulfur donors, although the g_z and A_z values are similar to complexes with N_2O_2 donor atoms. In addition, the large g- and A-anisotropy in the equatorial plane is a consequence of the different bond lengths and bond angles for the equatorial ligating atoms (Table II). Unfortunately, a detailed analysis of the g and A values in terms of molecular orbital parameters[52] is not possible as the $^2B_2 \rightarrow {}^2E$ and the $^2B_2 \rightarrow {}^2B_1$ transitions are hidden underneath a charge transfer band at around 350 to 390 nm (see Experimental Section). However, qualitatively, the low values of A_x and A_y may be explained by an increased interaction between the metal based d_{xy}, d_{yz} and the appropriate ligand p_z orbitals.

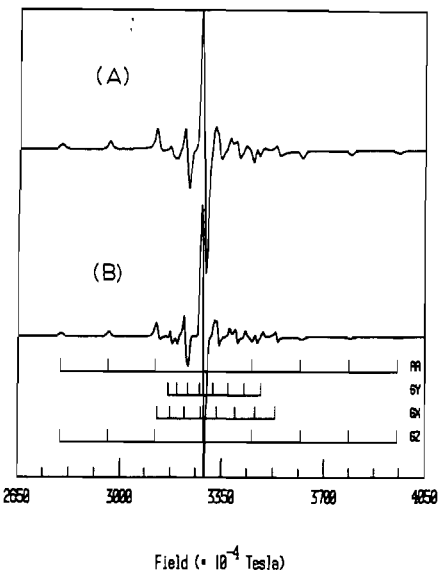

Figure 3. Frozen solution EPR spectra of [VO(pycac)] in chloroform: (A) experimental spectrum, $\nu = 9.25062$ GHz; (B) computer simulation, LSE = 1.669×10^{-3}.

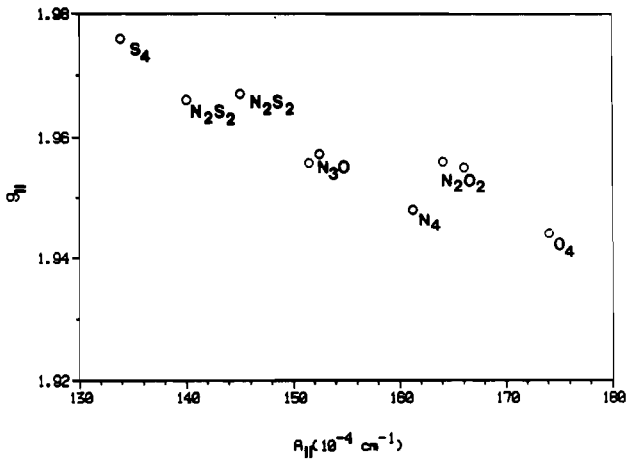

Figure 4. A correlation plot of $A_{\parallel}$ versus $g_{\parallel}$ for a series of oxovanadium(IV) complexes (listed in Table IV) with differing equatorial ligand field strengths.

(52) Money, J. K.; Folting, K.; Huffman, J. C.; Collison, D.; Temperley, J.; Mabbs, F. E.; Christou, G. *Inorg. Chem.* **1986**, *25*, 4583.

The expressions relating the hyperfine coupling constants to the molecular orbital parameters and the electronic transitions[52,53] reveal a correlation between A_i and g_i (where $i = x, y, z$) with equatorial ligand field donor types $VO(O_4)$, $VO(N_2O_2)$, $VO(N_4)$, $VO(N_2S_2)$, and $VO(S_4)$. The correlation between $A_\parallel$ and $g_\parallel$ with axially symmetric ligand fields has been used to identify the vanadium ion's coordination sphere in a number of metalloproteins.[15,54] Addition of the g_z and A_z values for [VO(pycac)] and [VO(pycbac)] to such a plot (Figure 4) shows that these complexes have an intermediate ligand field strength between (S_4 and N_2S_2) and O_4 donor types.

In the present study oxovanadium(IV) complexes with the unsymmetrical ligands $pycac^{2-}$ and $pycbac^{2-}$ have been prepared and structurally characterized. These complexes represent the first examples of oxovanadium(IV) complexes containing a vanadium–amide linkage. EPR spectra reveal an orthorhombic ligand field about the central metal ion which is consistent with the structural data. The electrochemical measurements reveal reversible one-electron redox processes involving vanadium in the oxidation states of V, IV, and III. Isolation and characterization of these species are currently underway.

Relationship to Biological Systems. In biological systems the available ligand atoms are sulfur (sulfide, thiolate), nitrogen (amide and amine), and oxygen (oxide, hydroxide, water, alcoholate, phenolate, carboxylate, hydroxamate). Although the interactions of vanadium with oxygen and sulfur atoms are becoming better understood, little is yet known about the ligation of nitrogeneous ligands to vanadium and in particular vanadium–amide binding.[17-20] The oxovanadium(IV) is a useful paramagnetic probe (vanadate is a useful diamagnetic probe) of protein structure and is therefore important to ascertain the nature of its amino acid and peptide (or peptide like, e.g., H_2pycac) complexes and the preference exhibited by oxovanadium(IV) (or vanadate) for various potential chelating combinations with those amino acids and peptide groups.

Despite the contribution of Gillard[58] et al. in determining the interactions of a number of amino acids with oxovanadium(IV), more work in this area is still required, particularly as there is often controversy about the stability constants of vanadium–amino acids. For example Crans[19] et al. reported the log $k[M^-]$ for VO^{2+}–glycine (1:1 complex) to be 3.70, while Fabian[59] et al. and Tomiyask[60] et al. reported this value to be 6.51 and 6.23, respectively. Efforts to isolate and characterize vanadium–amino acid compounds have so far proved unsuccessful suggesting that the interaction between vanadium and amino acids may in fact be very weak. A number of vanadium *N*-peptide interactions have been claimed but without full characterization of the resulting species.

The work herein adds substantial data to the chemistry of vanadium–amide binding and is therefore relevant to the biochemistry of this element. Despite a few investigations concerned with the coordination of V(III), V(IV), and V(V) to different proteins, little is known about the coordination environment of vanadium in protein matrix. In order to model potential binding sites we have investigated the complexation of oxovanadium(IV) by small molecules containing an amide (peptide) bond and a pyridine nitrogen (which closely resembles with the histidine nitrogen). It is obvious from the crystallographic data presented in this paper that there is a strong bond between vanadium-deprotonated amide nitrogen justifying previous claims[17-20,61] and paving the way for further research in this area. In our laboratory we are studying the interactions of V(III), V(V), and of course V(IV) with different amino acids and peptides (or peptide-like compounds) in an attempt to provide a better understanding of vanadium protein binding.

Acknowledgment. We wish to thank Professor A. Bond and Dr. G. Lawrance for helpful discussions on the electrochemical aspects of this study, Dr. P. F. Kelly for useful discussions, and P. Kirkos for the design and preparation of some figures within this paper.

Registry No. Hpycan, 90209-82-8; Hpyca, 90209-81-7; H_2pycac, 141170-90-3; H_2pycbac, 141170-91-4; [VO(pycac)], 141170-92-5; [VO(pybac)], 141170-93-6; $[VO(pycac)]^+$, 141170-94-7; $[VO(pycac)]^-$, 141170-95-8; $[VO(pybac)]^+$, 141170-96-9; $[VO(pycbac)]^-$, 141170-97-0; $[VO(pycbac)]^{2-}$, 141170-98-1; picolinic acid, 98-98-6; *o*-nitrophenol, 88-75-5; pentane-2,4-dione, 123-54-6; 1-phenylbutane-1,3-dione, 2550-26-7; bis(pentane-2,4-dionato)oxovanadium(IV), 3153-26-2.

Supplementary Material Available: Listings of positional parameters ($\times 10^4$) of non-H atoms for [VO(pycac)] (a-form) (Table S1), positional parameters ($\times 10^4$) of non-H atoms for [VO(pycac)] (b-form) (Table S2), positional parameters ($\times 10^4$) of non-H atoms for [VO(pycbac)] (Table S3), positional and isotropic thermal parameters of the hydrogen atoms (Table S4), anisotropic thermal parameters of the non-H atoms (Table S5), bond lengths and bond angles (Table S6), and infrared spectral data for the oxovanadium(IV) complexes and their corresponding ligands (Table S7) (13 pages); listings of the observed and calculated structure factors for the three oxovanadium(IV) complexes (Tables S8–S10) (80 pages). Ordering information is given on any current masthead page.

(53) Kivelson, D.; Lee, S.-K. *J. Chem. Phys.* **1964**, *41*, 1896.
(54) Sakurai, H.; Hirata, J.; Michibata, H. *Biochem. Biophys. Res. Commun.* **1987**, *149*, 411.
(55) Jezierski, A.; Raynor, J. B. *J. Chem. Soc., Dalton Trans.* **1981**, 1.
(56) Brand, S. G. MSc. Thesis, The University of Queensland, 1987.
(57) Dutton, J. C.; Fallon, G. D.; Murray, K. S. *Inorg. Chem.* **1988**, *27*, 34.
(58) (a) Pessoa, J. C.; Boas, L. F. V.; Gillard, R. D.; Lancashire, R. J. *Polyhedron* **1988**, *7*, 1245. (b) Pessoa, J. C.; Boas, L. F. V.; Gillard, R. D. *Polyhedron* **1989**, *8*, 1173. (c) Pessoa, J. C.; Marques, R. L.; Boas, L. F. V.; Gillard, R. D. *Polyhedron* **1990**, *9*, 81. (d) Pessoa, J. C.; Boas, L. F. V.; Gillard, R. D. *Polyhedron* **1990**, *9*, 2101.
(59) Fabian, S.; Nagypal, I. *Inorg. Chim. Acta* **1982**, *62*, 193.
(60) Tomiyasu, H.; Gordon, G. *J. Coord. Chem.* **1973**, *3*, 47.
(61) Kuwahara, J.; Suzuki, T.; Sugiura, Y. *Biochem. Biophys. Res. Commun.* **1985**, *129*, 368.